Supplementary Information

for

Facile Calixarene-based Sensor Array Strategy for Quality Evaluation of Yinxing Mihuan Oral Solution

Kejing Niu [a,#], Mengyu Ye [a,#], Yun Lyu [a], Wenqian Cheng [a], Shaoqing He [d], Dan Liu [c,*], Huijuan Yu [a,b,*]

[a] State Key Laboratory of Chinese Medicine Modernization, State Key Laboratory of Component-based Chinese Medicine, Tianjin University of Traditional Chinese Medicine, Tianjin, 301617, China.

[b] Haihe Laboratory of Modern Chinese Medicine, Tianjin, 301617, China.

[c] Department of Pharmacy, 967th Hospital of the Joint Logistics Support Force of the Chinese People's Liberation Army, Dalian, Liaoning, 116011, China.

[d] Xi'an Buchang TCM Cardiovascular and Cerebrovascular Hospital, Xi'an, Shaanxi, 710082, China.

[*] Corresponding author. E-mail addresses: dlld3836@163.com (D. Liu); huijuanyu@tjutcm.edu.cn (H. Yu).

[#] Kejing Niu and Mengyu Ye contributed equally to this work.

1. Supporting information and raw data

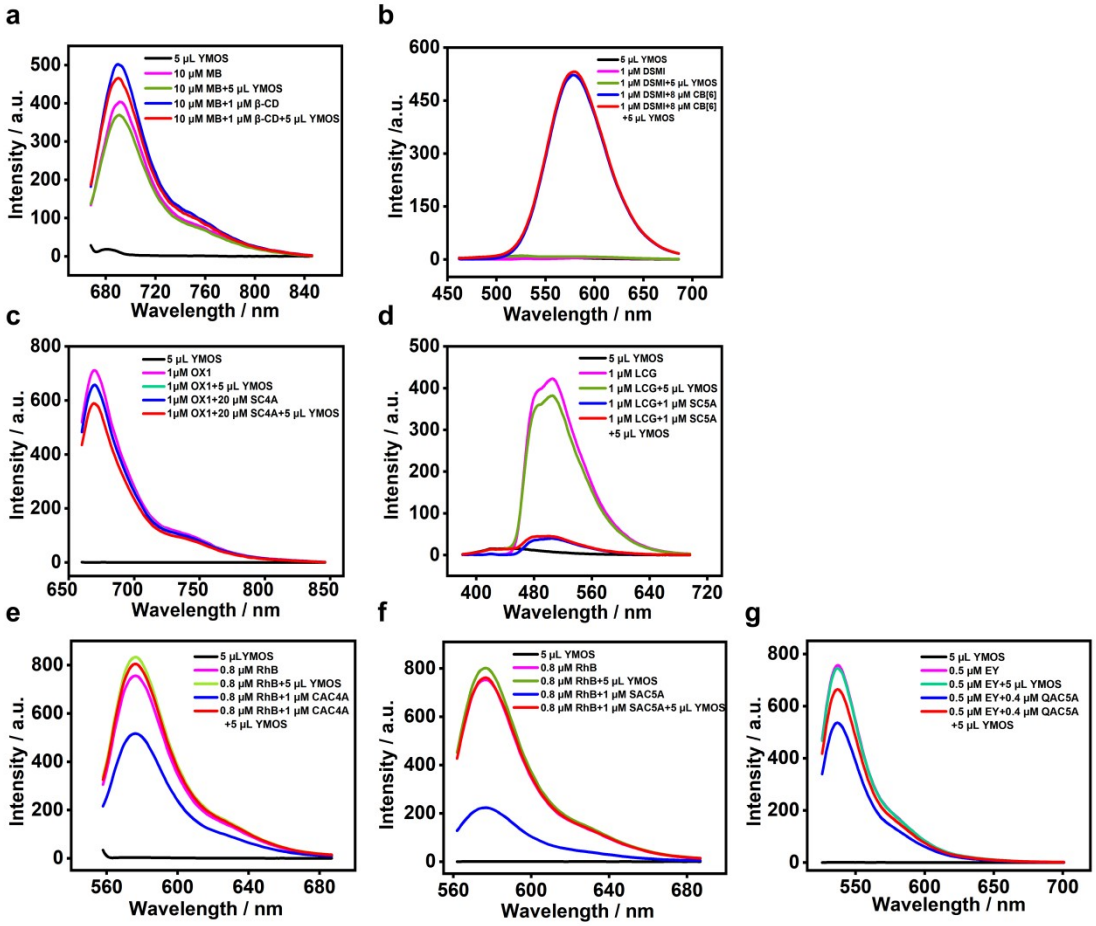

Figure S1. The fluorescence spectra of YMOS (5 μL), YMOS's impact on the fluorescence spectra of dyes, and the alterations in fluorescence of macrocycle•dye reporter pairs upon the addition of YMOS (5 μL) in HEPES buffer solution (10 mM, pH=7.4) at 25 °C. (a) *β*-CD•MB (1.0 μM/10.0 μM; λ_{ex} = 664 nm, λ_{em} = 688 nm), (b) CB[6]•DSMI (8.0 μM/1.0 μM; λ_{ex} = 450 nm, λ_{em} = 582 nm), (c) SC4A•OX1 (20.0 μM/1.0 μM; λ_{ex} = 648 nm, λ_{em} = 668 nm), (d) SC5A•LCG (1.0 μM/1.0 μM; λ_{ex} = 368 nm, λ_{em} = 505 nm), (e) CAC4A•RhB (1.0 μM/0.8 μM; λ_{ex} = 554 nm, λ_{em} = 576 nm), (f) SAC5A•RhB (1.0 μM/0.8 μM; λ_{ex} = 554 nm, λ_{em} = 576 nm), (g) QAC5A•EY (0.4 μM/0.5 μM; λ_{ex} = 517 nm, λ_{em} = 537 nm).

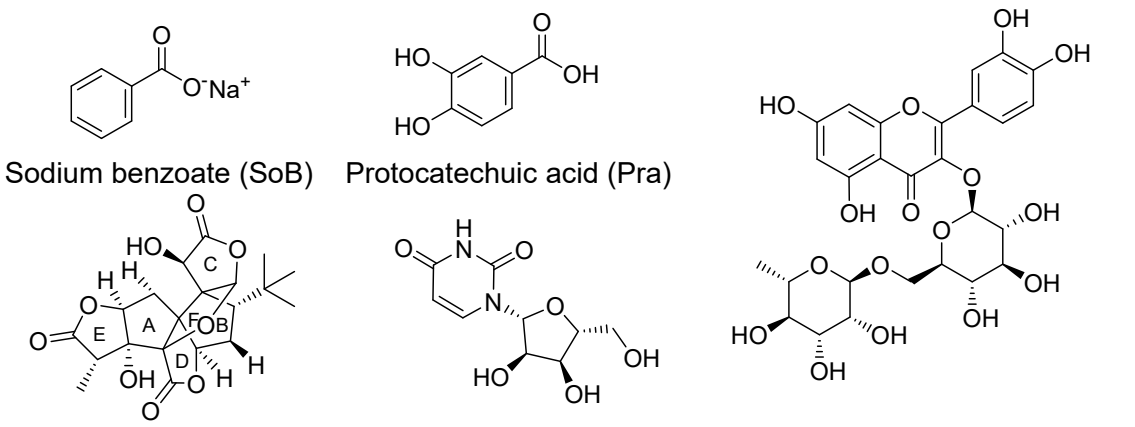

Figure S2. Chemical structures of the focused compounds from YMOS.

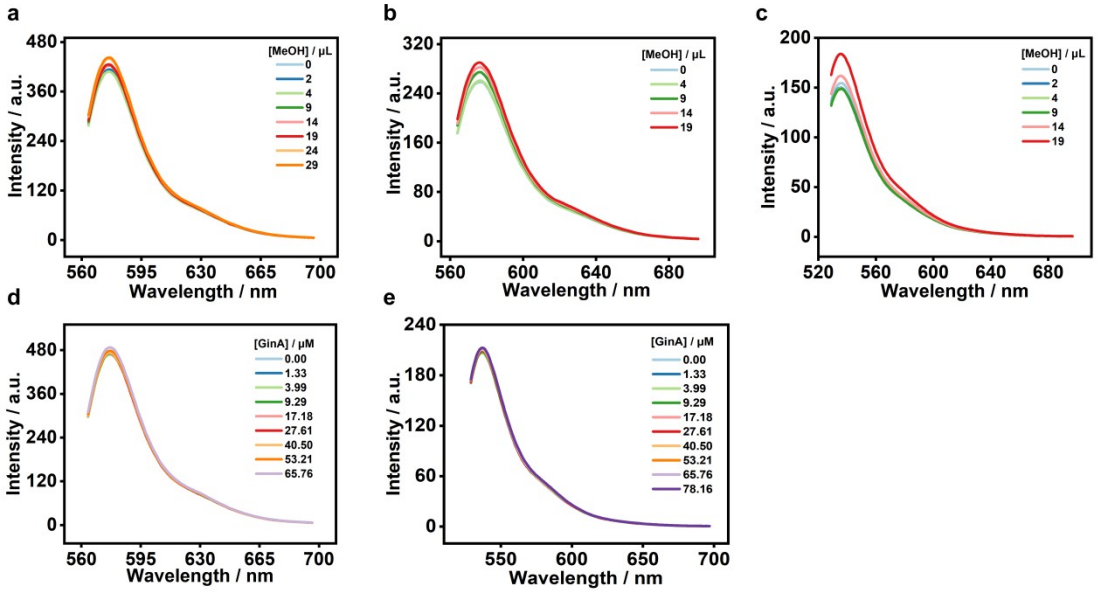

Figure S3. Fluorescence spectra of CA•dye (CAC4A•RhB, SAC5A•RhB, and QAC5A•EY) titrated by MeOH and dyes (RhB and EY) titrated by GinA in HEPES buffer solution (10 mM, pH 7.4) at 25 °C. (a) Fluorescence spectra of CAC4A•RhB (1.0 μM/0.8 μM) reporter pair titrated by MeOH (up to 29 μL) at λ_{ex} = 554 nm and λ_{em} = 576 nm. (b) Fluorescence spectra of SAC5A•RhB (1.0 μM/0.8 μM) reporter pair titrated by MeOH (up to 19 μL) at λ_{ex} = 554 nm and λ_{em} = 576 nm. (c) Fluorescence spectra of QAC5A•EY (0.4 μM/0.5 μM) reporter pair titrated by MeOH (up to 19 μL) at λ_{ex} = 517 nm and λ_{em} = 537 nm. (d) Fluorescence spectra of RhB (0.8 μM) titrated by GinA (up to 65.76 μM) at λ_{ex} = 554 nm and λ_{em} = 576 nm. (e) Fluorescence spectra of EY (0.5 μM) titrated by GinA (up to 78.16 μM) at λ_{ex} = 517 nm and λ_{em} = 537 nm.

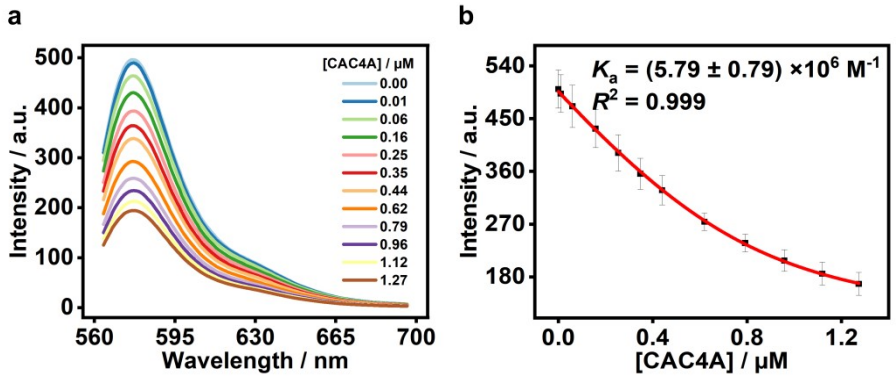

Figure S4. Direct fluorescence titration of RhB with CAC4A in HEPES buffer solution (10 mM, pH 7.4) at 25 °C. (a) Direct fluorescence titration of RhB (0.8 μM) with CAC4A (up to 1.27 μM) at λ_{ex} = 554 nm and λ_{em} = 576 nm. (b) The titration curve of RhB (0.8 μM) with CAC4A at λ_{em} =576 nm acquired by a 1:1 binding model (n = 3).

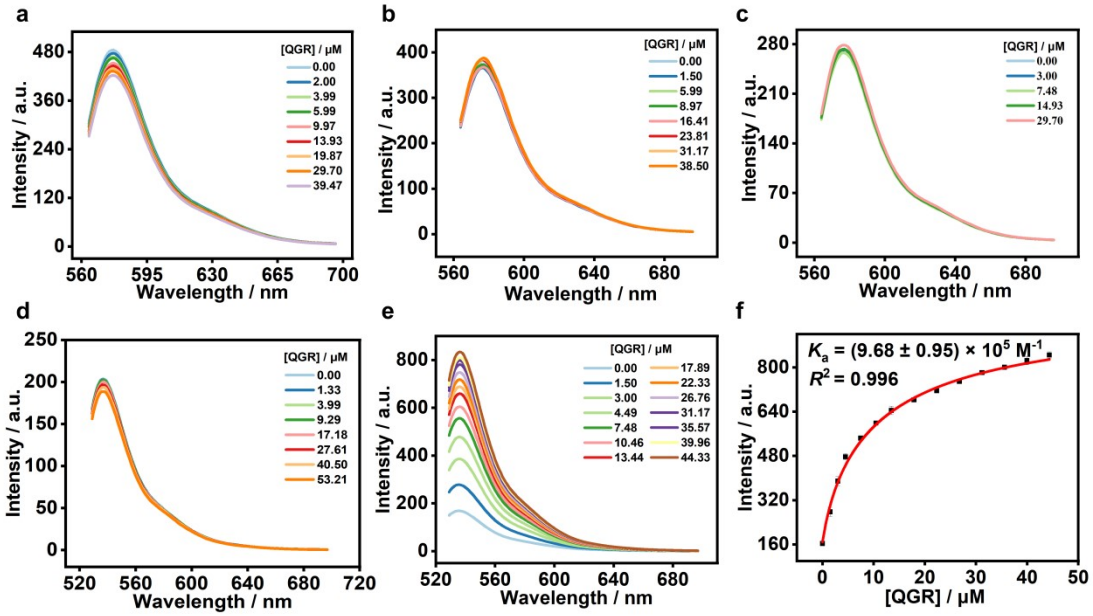

Figure S5. Fluorescence spectra of dyes (RhB and EY) titrated by QGR and competitive fluorescence titration of CA•dye (CAC4A•RhB, SAC5A•RhB, QAC5A•EY) reporter pairs with QGR in HEPES buffer solution (10 mM, pH 7.4) at 25 °C. (a) Fluorescence spectra of RhB (0.8 μM) titrated by QGR (up to 39.47 μM) at λ_{ex} = 554 nm and λ_{em} = 576 nm. (b) Competitive titration of CAC4A•RhB (1.0 μM/0.8 μM) reporter pair with QGR (up to 38.50 μM) at λ_{ex} = 554 nm and λ_{em} = 576 nm. (c) Competitive titration of SAC5A•RhB (1.0 μM/0.8 μM) reporter pair with QGR (up to 29.70 μM) at λ_{ex} = 554 nm and λ_{em} = 576 nm. (d) Fluorescence spectra of EY (0.5 μM) titrated by QGR (up to 53.21 μM) at λ_{ex} = 517 nm and λ_{em} = 537 nm. (e) Competitive titration of QAC5A•EY (0.4 μM/0.5 μM) reporter pair with QGR (up to 44.33 μM) at λ_{ex} = 517 nm and λ_{em} = 537 nm. (f) The titration curve of QAC5A•EY (0.4 μM/0.5 μM) with QGR at λ_{em} = 537 nm acquired by a 1:1 binding model (n = 3).

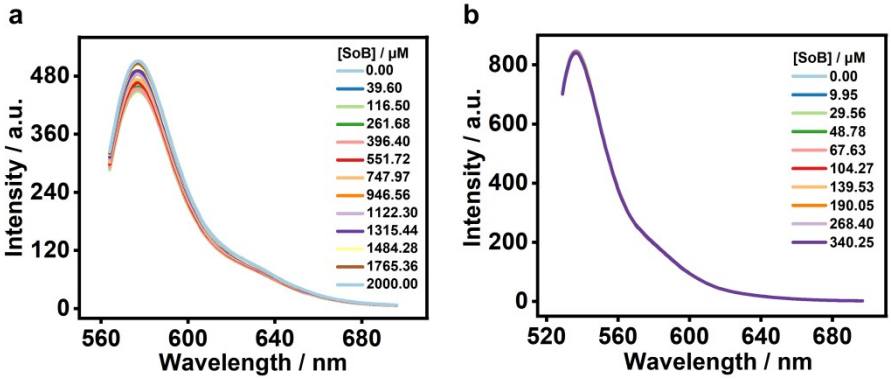

Figure S6. Fluorescence spectra of dyes (RhB and EY) titrated by SoB in HEPES buffer solution (10 mM, pH 7.4) at 25 °C. (a) Fluorescence spectra of RhB (0.8 μM) titrated by SoB (up to 2000 μM) at λ_{ex} = 554 nm and λ_{em} = 576 nm. (b) Fluorescence spectra of EY (0.5 μM) titrated by SoB (up to 340.25 μM) at λ_{ex} = 517 nm and λ_{em} = 537 nm.

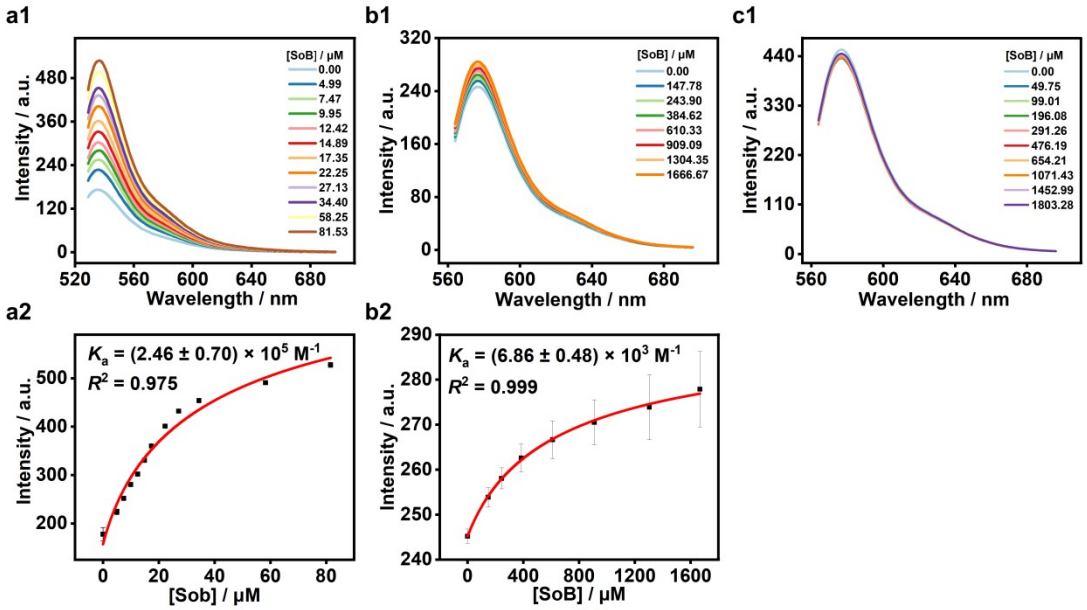

Figure S7. Competitive fluorescence titration of CA•dye (QAC5A•EY, SAC5A•RhB, CAC4A•RhB) reporter pairs with SoB in HEPES buffer solution (10 mM, pH 7.4) at 25 °C. (a1) Competitive fluorescence titration of QAC5A•EY (0.4 μM/0.5 μM) reporter pair with SoB (up to 81.53 μM) at λ_{ex} = 517 nm and λ_{em} = 537 nm. (a2) The titration curve of QAC5A (0.4 μM) with SoB at λ_{em} = 537 nm acquired by a 1:1 binding model (n = 3). (b1) Competitive fluorescence titration of SAC5A•RhB (1.0 μM/0.8 μM) reporter pair with SoB (up to 1666.67 μM) at λ_{ex} = 554 nm and λ_{em} = 576 nm. (b2) The titration curve of SAC5A (1.0 μM) with SoB at λ_{em} = 576 nm acquired by a 1:1 binding model (n = 3). (c1) Competitive fluorescence titration of CAC4A•RhB (1.0 μM/0.8 μM) reporter pair with SoB (up to 1803.28 μM) at λ_{ex} = 554 nm and λ_{em} = 576 nm.

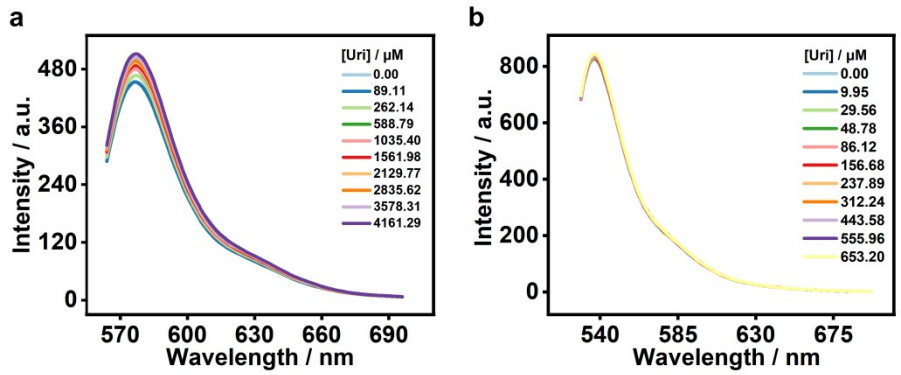

Figure S8. Fluorescence spectra of dyes (RhB and EY) titrated by Uri in HEPES buffer solution (10 mM, pH 7.4) at 25 °C. (a) Fluorescence spectra of RhB (0.8 μM) titrated by Uri (up to 4161.29 μM) at λ_{ex} = 554 nm and λ_{em} = 576 nm. (b) Fluorescence spectra of EY (0.5 μM) titrated by Uri (up to 653.20 μM) at λ_{ex} = 517 nm and λ_{em} = 537 nm.

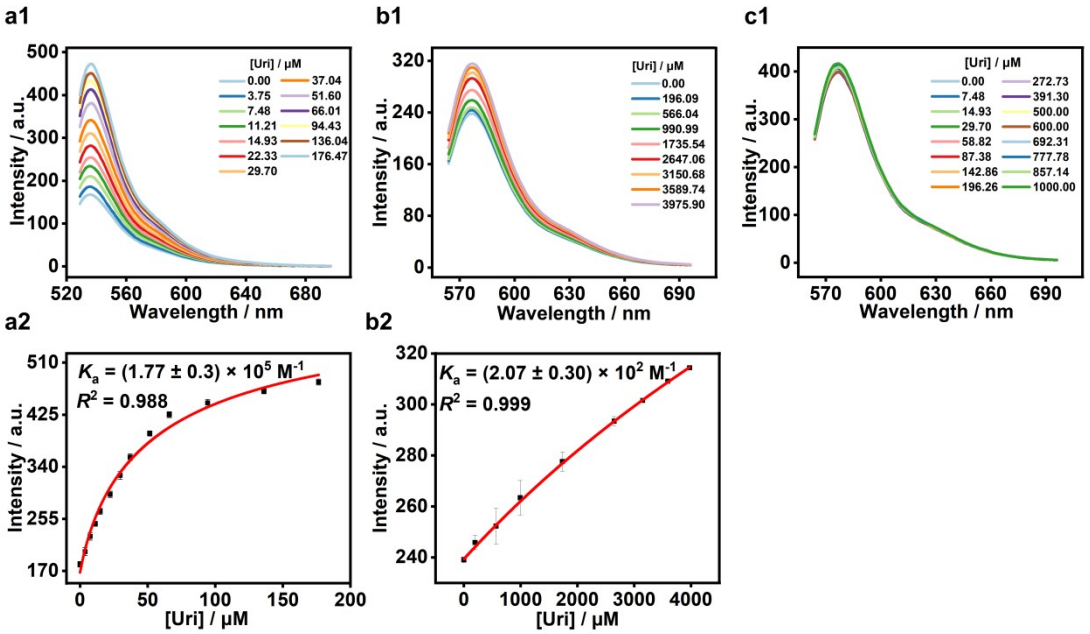

Figure S9. Competitive fluorescence titration of CA•dye (QAC5A•EY, SAC5A•RhB, CAC4A•RhB) reporter pairs with Uri in HEPES buffer solution (10 mM, pH 7.4) at 25 °C. (a1) Competitive fluorescence titration of QAC5A•EY (0.4 μM/0.5 μM) reporter pair with Uri (up to 176.47 μM) at λ_{ex} = 517 nm and λ_{em} = 537 nm. (a2) The titration curve of QAC5A•EY (0.4 μM/0.5 μM) with Uri at λ_{em} = 537 nm acquired by a 1:1 binding model (n = 3). (b1) Competitive fluorescence titration of SAC5A•RhB (1.0 μM/0.8 μM) reporter pair with Uri (up to 3975.90 μM) at λ_{ex} = 554 nm and λ_{em} = 576 nm. (b2) The titration curve of SAC5A•RhB (1.0 μM/0.8 μM) with Uri at λ_{em} = 576 nm acquired by a 1:1 binding model (n = 3). (c1) Competitive fluorescence titration of CAC4A•RhB (1.0 μM/0.8 μM) reporter pair with Uri (up to 1000 μM) at λ_{ex} = 554 nm and λ_{em} = 576 nm.

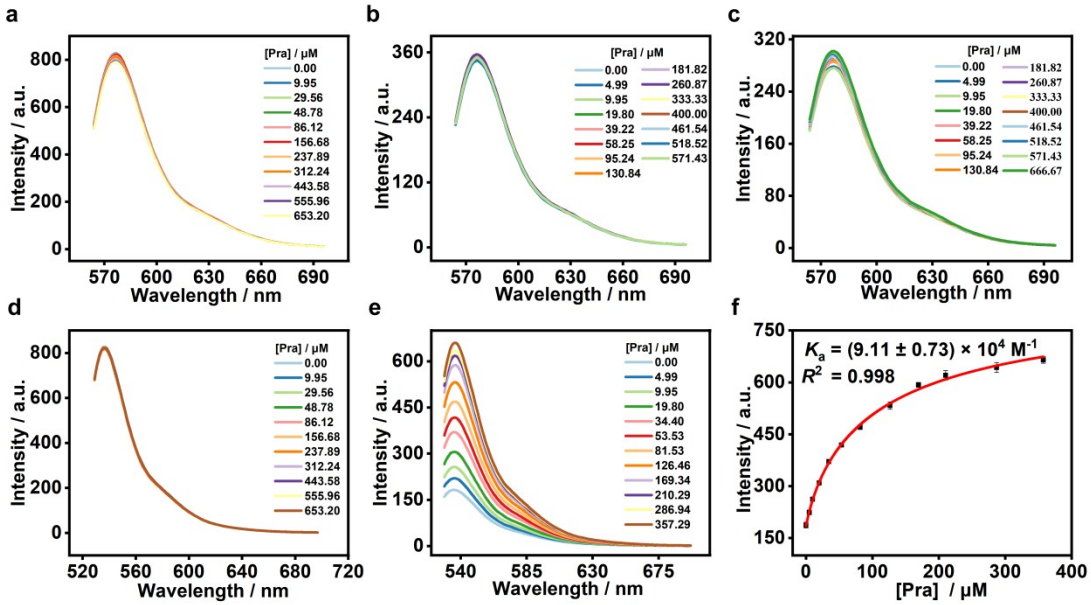

Figure S10. Fluorescence spectra of dyes (RhB and EY) titrated by Pra and competitive titration of CA•dye (CAC4A•RhB, SAC5A•RhB, QAC5A•EY) reporter pairs with Pra in HEPES buffer solution (10 mM, pH 7.4) at 25 °C. (a) Fluorescence spectra of RhB (0.8 μM) titrated by Pra (up to 653.20 μM) at λ_{ex} = 554 nm and λ_{em} = 576 nm. (b) Competitive fluorescence titration of CAC4A•RhB (1.0 μM/0.8 μM) reporter pair with Pra (up to 571.43 μM) at λ_{ex} = 554 nm and λ_{em} = 576 nm. (c) Competitive fluorescence titration of SAC5A•RhB (1.0 μM/0.8 μM) reporter pair with Pra (up to 666.67 μM) at λ_{ex} = 554 nm and λ_{em} = 576 nm. (d) Fluorescence spectra of EY (0.5 μM) titrated by Pra (up to 653.20 μM) at λ_{ex} = 517 nm and λ_{em} = 537 nm. (e) Competitive titration of QAC5A•EY (0.4 μM/0.5 μM) reporter pair with Pra (up to 357.29 μM) at λ_{ex} = 517 nm and λ_{em} = 537 nm. (f) The titration curve of QAC5A•EY (0.4 μM/0.5 μM) with Pra at λ_{em} = 537 nm acquired by a 1:1 binding model (n = 3).

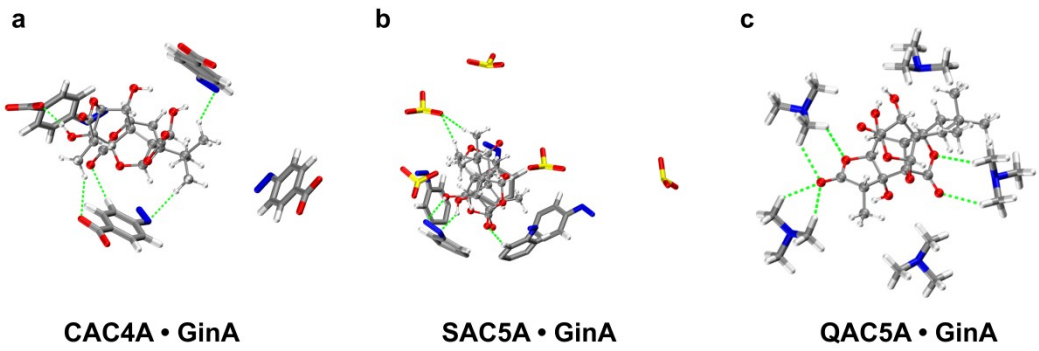

Figure S11. The hydrogen bond (green lines) mode of CAC4A•GinA, SAC5A•GinA, and QAC5A•GinA complexes at the B3LYP-D3 (BJ)/6-31G (d)/SMD (water) theoretical level (for the sake of clarity of CAC4A, SAC5A, and QAC5A, only the groups with hydrogen bonds with the analytes are shown)

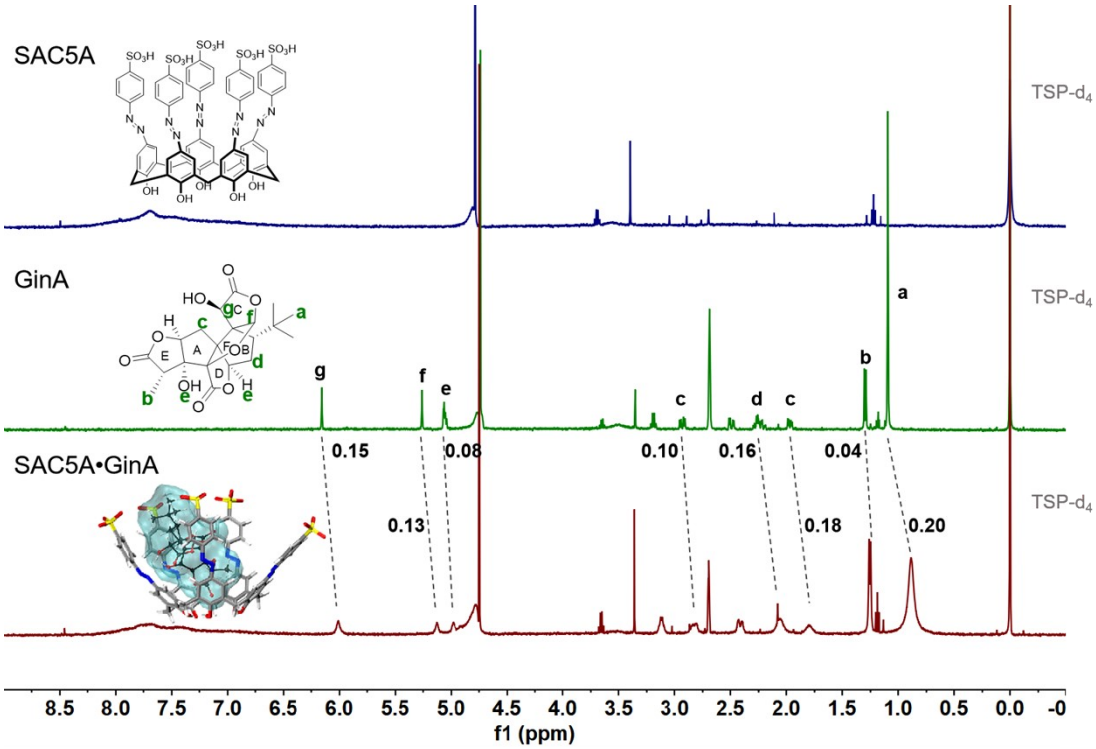

Figure S12. Elucidation of the SAC5A•GinA complex by ^{1}H-NMR spectroscopic analysis (500 MHz, D_2O, 298 K, internal reference standards: TSP-d_4).

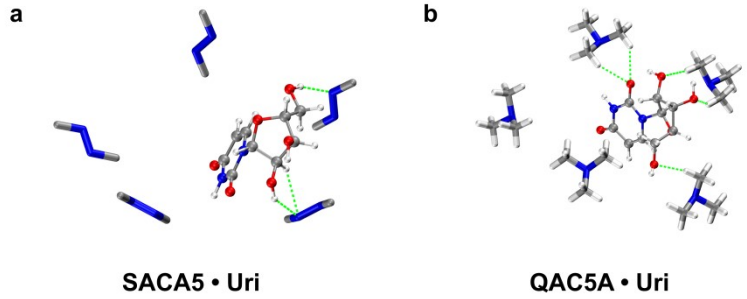

Figure S13. The hydrogen bond (green lines) mode of SAC5A•Uri (a) and QAC5A•Uri (b) complexes at the B3LYP-D3 (BJ)/6-31G (d)/SMD (water) theoretical level (for the sake of clarity of SAC5A and QAC5A, only the groups with hydrogen bonds with the analytes are shown)

Table S1. Association constant (K_a/M^{-1}) between the macrocyclic host and the analyte (n = 3).

Analyte \ Host	CAC4A	SAC5A	QAC5A
QGR	–	–	$(9.68\pm0.95)\times10^5$
SoB	–	$(6.86\pm0.48)\times10^3$	$(2.46\pm0.70)\times10^5$
GinA	$(4.43\pm0.77)\times10^4$	$(6.35\pm2.45)\times10^5$	$(5.50\pm1.52)\times10^4$
Uri	–	$(2.07\pm0.30)\times10^2$	$(1.77\pm0.30)\times10^5$
Pra	–	–	$(9.11\pm0.73)\times10^4$

" – " represents no obvious binding affinity.

Table S2. Calculation results of the binding energy (hartree) of host•analyte complexes.

Host•analyte	Single point energy (hartree)			ΔE
	E_{HA}	E_H	E_A	
CAC4A•GinA	-5024.79	-3495.80	-1528.87	-0.12
SAC5A•GinA	-8075.33	-6546.34	-1528.88	-0.11
QAC5A•GinA	-5304.94	-3775.97	-1528.88	-0.09
SAC5A•Uri	-7457.48	-6546.36	-911.04	-0.08
QAC5A•Uri	-4687.11	-3775.98	-911.04	-0.09

Table S3. Summary of the non-covalent interactions between Host•Analyst

Host•Analyst	interactions	Groups in host	Groups in analyst
CAC4A•GinA	O–H···O	–COOH	–OH
	C–H···O	–COOH	$–CH_3$
	Ar–H···O	Ar–H	–C=O
	C–H···N	–N=N–	$–C(CH_3)_3$
	O–H···π	Ar	–OH
	π–π	–N=N– and Ar	–O–
SAC5A•GinA	O–H···N	–N=N–	–OH
	C–H···O	$–SO_3H$	$–CH_3$
	Ar–H···O	Ar–H	–C=O
	O–H···π	Ar	–OH
	C–H···π	Ar	–CH–
	π–π	–N=N– and Ar	–O–
QAC5A•GinA	C–H···O	$–N(CH_3)_3$	–C=O and –O–
	C–H···π	Ar	–CH–
	π–π	Ar	–C=O and –O–
SAC5A•Uri	O–H···N	–N=N–	–OH
	C–H···N	–N=N–	–CH–
	N–H···π	Ar	–NH–
	π–π	–OH	–C=O
QAC5A•Uri	C–H···O	$–N(CH_3)_3$	–OH and –C=O
	N–H···π	Ar	–NH–
	C–H···π	Ar	–CH–
	π–π	Ar	–C=O

Table S4. The normalized I/I_0 ($E_{m\text{-}k}$) of 12 batches of qualified YMOS samples determined by different sensor units (n=3).

Em-k / Batches	CAC4A•RhB			SAC5A•RhB			QAC5A•EY		
	1	2	3	1	2	3	1	2	3
YM1	0.9364	0.9391	0.9488	0.9024	0.9251	0.9066	0.9188	0.9454	0.9515
YM2	0.9479	0.9445	0.9343	0.9099	0.9118	0.8996	0.9313	0.9459	0.9248
YM3	0.9576	0.9453	0.9330	0.9088	0.9033	0.9027	0.9657	0.9263	0.9468
YM4	0.9772	0.9315	0.9345	0.9102	0.9070	0.9051	0.9576	0.9475	0.9395
YM5	0.9462	0.9287	0.9546	0.9257	0.9027	0.9126	0.9529	0.9664	0.9647
YM6	0.9778	0.9441	0.9670	0.9186	0.9015	0.9110	0.9363	0.9819	0.9460
YM7	0.9861	0.9717	1.000	0.9808	0.9890	0.9764	0.9447	0.9570	0.9647
YM8	0.9805	0.9677	0.9599	0.9777	0.9770	0.9679	0.9435	0.9310	0.9450
YM9	0.9743	0.9691	0.9765	0.9677	0.9823	0.9840	0.9592	0.9566	0.9627
YM10	0.9715	0.9779	0.9631	0.9883	0.9852	0.9850	0.9613	0.9704	0.9633
YM11	0.9765	0.9665	0.9701	0.9833	0.9755	0.9705	1.000	0.9901	0.9624
YM12	0.9685	0.9783	0.9751	0.9751	0.9830	1.000	0.9469	0.9493	0.9619

Table S5. The "spider-web" area (*S*) for 12 batches of qualified YMOS samples (*n*=3).

Batches \ *S*	*S*1	*S*2	*S*3	$\overline{S}$	Standard deviation
YM1	1.097	1.139	1.137	1.125	0.024
YM2	1.123	1.133	1.098	1.118	0.018
YM3	1.157	1.111	1.117	1.129	0.025
YM4	1.168	1.120	1.115	1.134	0.029
YM5	1.152	1.129	1.157	1.146	0.015
YM6	1.158	1.153	1.151	1.154	0.004
YM7	1.223	1.229	1.248	1.233	0.013
YM8	1.215	1.193	1.191	1.200	0.013
YM9	1.215	1.221	1.233	1.223	0.009
YM10	1.231	1.242	1.223	1.232	0.009
YM11	1.264	1.241	1.216	1.241	0.024
YM12	1.206	1.223	1.245	1.224	0.020

Table S6. The fluorescence response of QAC5A•EY exposed to self-made YMOS samples (*n*=6).

I/I_0	1		2		3		Average	RSD (%)
	1-1	1-2	2-1	2-2	3-1	3-2		
0:30	3.017	3.085	3.261	3.090	3.186	3.146	3.131	2.5%
1:30	4.331	3.978	4.118	4.206	4.395	4.201	4.205	3.2%
3:30	5.178	4.907	4.982	4.805	5.194	5.063	5.021	2.8%
6:30	6.522	6.632	6.236	6.238	6.271	6.260	6.360	2.5%

Table S7 Application of sensing technology in quality evaluation of TCM

Analyte	Method	Material	Principle	Testing time/volume	Advantages	Conclusion	Ref.
Radix Codonopsis	Electronic sensing	Mental oxide semiconductors	The study employed electronic tongue technology to obtain sweetness values, and captured odor fingerprint information through an electronic nose.	130 s per sample in electronic tongue test, 720 s per sample in electronic nose test	Rapid, simple and accurate	The alcohol-soluble extract content and polysaccharide extract, as well as taste and color of *Radix Codonopsis* were predicted.	[1]
Polygonatum Sibiricum Red.	Chemsensor	4-Hydrazino-1,8-naphthalimide (HAN)	The synthesized HAN exhibited a turn-on fluorescence response toward monosaccharide with a bright orange fluorescence under UV radiation.	12 min per sample/10 μL	Excellent precision and good accuracy	The quality control of polysaccharide and qualtification of four monosaccharides from *P. sibiricum*	[2]

						Red. Polysaccharide were simultaneously performed .	
Baicalin (Bn) and baicalein (Be)	electrochemical sensor	Biochar (BC)/ZIF-67/$MnCo_2O_4$ composite	The BC/ZIF-67/$MnCo_2O_4$ displayed the increased electroactive surface area, enhanced electrocatalytic properties, and improved electrical conductivity of the catalyst, facilitating improved sensitivity and selectivity.	–	Superior sensitivity, selectivity, accuracy, and practicality	The content of baicalin and baicalein were simultaneously detected.	[3]
Bulbus Lilii	near-infrared spectroscopy sensor	Carbon dottetramethoxypo-rphyrin nanocomposite	The potential of carbon dot-tetramethoxyporphyrin nanocomposite-based nano-effect near-infrared spectroscopy sensor combined with chemometric method was investigated for identifing lily from different geographical origins.	–	Simple, rapid and accurate	The geographical origin of lily was distinguished.	[4]
Licorice	Colorimetric	Iron oxide	The peroxidase-like activities of three iron	40 min per	Easy-to-use,	Glycyrrhizic acid,	[5]

	sensor array	nanozymes	oxide nanozymes (Fe_2O_3, Fe_3O_4, His-Fe_3O_4) could be inhibited by the competitive effects of active substances of licorice, which resulted in the inability of H_2O_2 to prevent fading of TMB.	sample /5 μL	effective and sensitive	liquiritin, licochalcone A and isolicoflavonol were identified as the active compounds.	
Qufeng Zhitong Capsule (QZC)	Fluorescence sensor array	Calixarenes/ Calixarenes•dyes	The molecular recognitions between azocalixarenes and the compounds of QZC are transduced through the fluorescence signal output of the QZC itself or the applied indicator.	10 min per sample/2.5 μL	Facile, rapid, and less technically demanding	Standard fingerprint of qualified sample was constructed for quality evaluation of QZC.	[6]
Yinxing Mihuan Orial Solution (YMOS)	Fluorescence sensor array	Calixarenes•dyes	Using indicator displacement assay (IDA), the molecular recognitions between calixarenes and the tested compounds from YMOS were converted into multi-fluorescence signals by extruding the indicators from their respective hosts.	10 min per sample/5 μL	Simple sample preparation and environmental friendliness	The inter-batch consistency evaluation and feeding ratio monitoring of YMOS were realized.	Present work

References

1. X. Guo, R. Yang, Y. Wang, J. Wang, Y. Wang, H. Zou and Y. Yan, Prediction of Chemical Composition and Sensory Information of Codonopsis Radix Based on Electronic Nose, *Molecules*, 2025, **30**, 1146.
2. Z. Wang, Q. Sun, Y. Zhao, J. Du and B. Wang, Synthesis of naphthalimide-type chemsensor and its application in quality evaluation for polygonatum sibiricum Red, *Frontiers in Chemistry*, 2022, **10**, 969014.
3. X. Zhang and R. Liu, An ultrasensitive electrochemical sensor for the simultaneous detection of baicalin and baicalein in pharmaceuticals and serum samples, *Talanta*, 2025, **285**, 127414.
4. W. Long, Z. Hu, L. Wei, H. Chen, T. Liu, S. Wang, Y. Guan, X. Yang, J. Yang and H. Fu, Accurate identification of the geographical origins of lily using near-infrared spectroscopy combined with carbon dot-tetramethoxyporphyrin nanocomposite and chemometrics, *Spectrochim. Acta A Mol. Biomol. Spectrosc.*, 2022, **271**, 120932.
5. X. Yuan, S. Cheng, L. Chen, Z. Cheng, J. Liu, H. Zhang, J. Yang and Y. Li, Iron oxides based nanozyme sensor arrays for the detection of active substances in licorice, *Talanta*, 2023, **258**, 124407.
6. J. H. Tian, Y. L. Lin, J. J. Li, R. Ma, H. Yu, Y. Wang, X. Y. Hu and D. S. Guo, Supramolecular fluorescence sensing for quality evaluation of traditional Chinese medicine, *Arab. J. Chem.*, 2023, **16**, 104974.